

## THE LYMAN- $\alpha$ FOREST OF THE QSO IN THE HUBBLE DEEP FIELD SOUTH<sup>1</sup>

S. SAVAGLIO<sup>1,2</sup>, H. C. FERGUSON<sup>1</sup>, T. M. BROWN<sup>3</sup>, B. R. ESPEY<sup>1,2</sup>, K. C. SAHU<sup>1</sup>, S. A. BAUM<sup>1</sup>, C. M. CAROLLO<sup>4</sup>, M. E. KAISER<sup>4</sup>, M. STIAVELLI<sup>1,2,5</sup>, R. E. WILLIAMS<sup>1</sup>, J. WILSON<sup>1</sup>

<sup>1</sup> Space Telescope Science Institute, 3700 San Martin Drive, Baltimore, MD21218, USA

<sup>2</sup> On assignment from the Space Science Department of the European Space Agency

<sup>3</sup> Laboratory for Astronomy & Solar Physics, Code 681, NASA/GSFC, Greenbelt, MD 20771

<sup>4</sup> Johns Hopkins University, 3701 San Martin Dr., 21218 MD, USA

<sup>5</sup> Scuola Normale Superiore, Piazza dei Cavalieri 7, I56126, Pisa, Italy

*Draft version January 1, 2018*

### ABSTRACT

The quasar in the Hubble Deep Field South (HDFS), J2233-606 ( $z_{em} = 2.23$ ) has been exhaustively observed by ground based telescopes and by the STIS spectrograph on board the Hubble Space Telescope (HST) at low, medium and high resolution in the spectral interval from 1120 Å to 10000 Å. The combined data give continuous coverage of the Lyman- $\alpha$  forest from redshift 0.9 to 2.24. This very large base-line represents a unique opportunity to study in detail the distribution of clouds associated with emitting structures in the field of the quasar and in nearby fields already observed as part of the HDFS campaign. Here we report the main properties obtained from the large spectroscopic dataset available for the Ly $\alpha$  clouds in the intermediate redshift range 1.20 - 2.20, where our present knowledge has been complicated by the difficulty in producing good data. The number density is shown to be higher than what is expected by extrapolating the results from both lower and higher redshifts:  $63 \pm 8$  lines with  $\log N_{HI} \geq 14.0$  are found (including metal systems) at  $\langle z \rangle = 1.7$ , to be compared with  $\sim 40$  lines predicted by extrapolating from previous studies. The redshift distribution of the Lyman- $\alpha$  clouds shows a region spanning  $z \simeq 1.383 - 1.460$  (comoving size of  $94 h_{65}^{-1}$  Mpc,  $\Omega_o = 1$ ) with a low density of absorption lines; we detect 5 lines in this region, compared with the 16 expected from an average density along the line of sight. The two point correlation function shows a positive signal up to scales of about  $3 h_{65}^{-1}$  Mpc and an amplitude that is larger for larger HI column densities. The average Doppler parameter is about  $27 \text{ km s}^{-1}$ , comparable to the mean value found at  $z > 3$ , thus casting doubts on the temperature evolution of the Ly $\alpha$  clouds.

*Subject headings:* cosmology: observations - quasars: absorption lines - quasars: individual: J2233-606

### 1. INTRODUCTION

A satisfactory connection between quasar absorption lines and galaxies close to the QSO line of sight has been provided so far only by relatively low redshift studies ( $z < 1.5$ ), as galaxies at high redshifts are much harder to observe. For  $z > 2$ , large samples of quasar absorption lines have been provided because at these redshifts the many strong UV lines are redshifted to the optical range, where very sensitive ground based observations can be obtained. However a complete picture in the whole observable redshift range is missing because of the lack of information at intermediate redshifts ( $1.5 < z < 2$ ).

With the advent of the high resolution UV spectrograph Space Telescope Imaging Spectrograph (STIS), a detailed study of the intermediate redshift Ly $\alpha$  forest and the connection to galaxy properties can now be obtained. Indeed, this was one of the motivations for the Hubble Deep Field South (HDFS). Much of the ground-based and HST HDFS campaign (Williams et al. 1999) has been devoted to the observations of the quasar J2233-606 ( $z_{em} = 2.23$ ) that lies in the STIS field (about 5 and 8 arcmin from the WFPC2 and NICMOS fields). The study of the quasar incorporates both spectroscopy (Sealy et al. 1998; Savaglio

1998; Outram et al. 1998; Ferguson et al. 1999) and imaging (Gardner et al. 1999).

Here we present the interesting features shown by the distribution of the Ly $\alpha$  clouds obtained by the fitting of the absorption lines in the redshift range  $1.20 < z < 2.20$  in the high and medium resolution spectra taken with STIS/HST (Ferguson et al. 1999<sup>2</sup>) and UCLES/AAT (Outram et al. 1998). The spectral resolution ranges from  $\text{FWHM} = 10 \text{ km s}^{-1}$  in the interval  $\lambda\lambda = 2670 - 3040 \text{ \AA}$ , to  $50 \text{ km s}^{-1}$  in  $\lambda\lambda = 3040 - 3530 \text{ \AA}$ , and to  $8.5 \text{ km s}^{-1}$  in  $\lambda\lambda = 3530 - 3900 \text{ \AA}$ .

### 2. THE DOPPLER PARAMETER AND THE COLUMN DENSITY REDSHIFT DISTRIBUTION

The line parameters have been obtained using the MIDAS package FITLYMAN (Fontana & Ballester 1995) in the spectral range  $2670 - 3900 \text{ \AA}$  through  $\chi^2$  minimization of Voigt profiles. At shorter wavelengths, the Lyman limit of the system at  $z \simeq 1.943$  absorbs a large fraction of the QSO flux, preventing the fit of absorption lines. The optical UCLES/AAT and STIS/HST spectra have been combined to simultaneously fit the Lyman series of the Ly $\alpha$  clouds and that gives more robust results than using

<sup>1</sup>Based on observations made with the NASA/ESA *Hubble Space Telescope* by the Space Telescope Science Institute, which is operated by AURA, Inc., under NASA contract NAS 5-26555.

<sup>2</sup>See also the HDFS web site at <http://www.stsci.edu/ftp/observing/hdf/hdfsouth/hdfs.html>

the Ly $\alpha$  line alone. Only the parameters of Ly $\alpha$  clouds at  $z < 1.60$  have been obtained using the Ly $\alpha$  absorption line alone. The redshift distribution of the Doppler parameters and of the column densities are shown in Fig. 1, together with the instrumental Doppler width and column density  $4\sigma$  detection limit for the Ly $\alpha$  lines. The sample does not include HI column densities associated with known metal systems, and lines close ( $z > 2.2$ ) to the quasar redshift that are considered to be affected by the ionization of the quasar. The number of identified intervening metal systems is 5. Three of them have a complex structure (for a total of 10 Ly $\alpha$  components) with HI column density in each system  $\log N_{\text{HI}} > 16$ . These clouds are presumably associated with galaxies and we consider them a different population of clouds with respect to lower HI column density clouds of the intergalactic medium, although many of them are presumably polluted of metals by nearby galaxies (Cowie & Songaila, 1998). Metal systems have been included in the sample only to compare the number density redshift evolution with previous studies at lower and higher redshifts (see section 3). The total number of Ly $\alpha$  clouds excluding metal systems is then 210. The reported  $4\sigma$  detection limit is determined by considering the error array of the spectra and does not take into account the line blending effect; at  $z > 1.7$  it is not very important because the line density at intermediate redshifts is relatively low, but it becomes particularly strong at lower redshifts, due to the presence of Lyman series lines of the higher redshift Ly $\alpha$  clouds that prevents detection of weak lines ( $N_{\text{HI}} < 10^{13.5} \text{ cm}^{-2}$ ). We therefore consider the completeness limit in the whole redshift range of  $N_{\text{HI}} \geq 10^{14} \text{ cm}^{-2}$ .

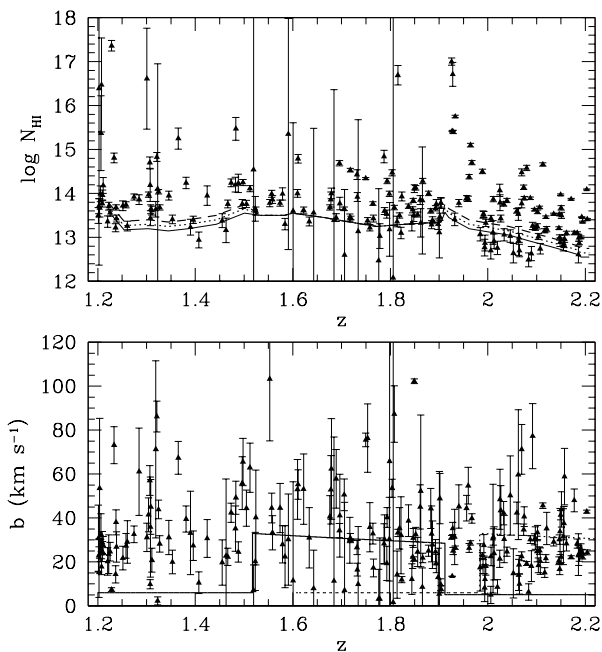


FIG. 1— The Doppler parameter (lower panel) and column density (upper panel) vs. redshift of the Ly $\alpha$  forest along the J2233–606 line of sight. The solid and dotted lines in the lower panel are the instrumental Doppler widths along the spectra for the Ly $\alpha$  and Ly $\beta$  forests respectively. The dashed, the dotted and the solid lines in the upper panel represent the  $4\sigma$  HI column density detection limit in the case of Doppler parameter of 40, 30 and 20  $\text{km s}^{-1}$  respectively.

Some interesting features can be noticed in the column density redshift distribution. There is a peak of high HI Ly $\alpha$  clouds at  $z = 1.92 - 1.99$  ( $\sim 60 h_{65}^{-1}$  Mpc comoving). A metal system with a  $z \simeq 1.943$  Lyman limit was first detected from the test STIS observations of the quasar. Therefore this peak might indicate the presence of a high density of galaxies at those redshifts. At lower redshifts (in the interval  $1.383 < z < 1.460$ ), we see a region with a low density of lines. The corresponding line density is  $dn/dz = 65$ , compared with an observed mean over the whole range of  $dn/dz = 210$  lines. There are no lines with HI column density larger than the completeness limit of  $10^{14} \text{ atoms/cm}^{-2}$ , while from the mean observed in the whole redshift range we would expect 4 lines. Although this is not statistically very significant, it is suggestive of the presence of a “void” of comoving size of  $94 h_{65}^{-1}$  Mpc. The redshift measurements of galaxies from multi-color ground observations and from the very deep STIS images of the field will probably confirm if this is real. The lack of Ly $\alpha$  lines can also be caused by a strong ionization of the clouds by the local UV radiation field, for instance in a quasar environment.

It is worth noting the decrement of lines going from the QSO redshift to  $\sim 1.38$ , shown by the histogram of the entire sample (Fig. 2). This effect disappears when selecting strong lines, and so it may be due to the detection limit variation along the spectrum. For smaller redshifts, the number of lines increases again. We notice that at  $z \simeq 1.335$ , a CIV system has been tentatively identified (Ferguson et al. 1999) and a quasar at a distance of about  $44.5''$  from the line of sight ( $\sim 300 h_{65}^{-1}$  kpc) has been found from the ground by EMMI/NTT observations (Tresse et al. 1998). This might also be an indication of an overdensity of objects at that redshift.

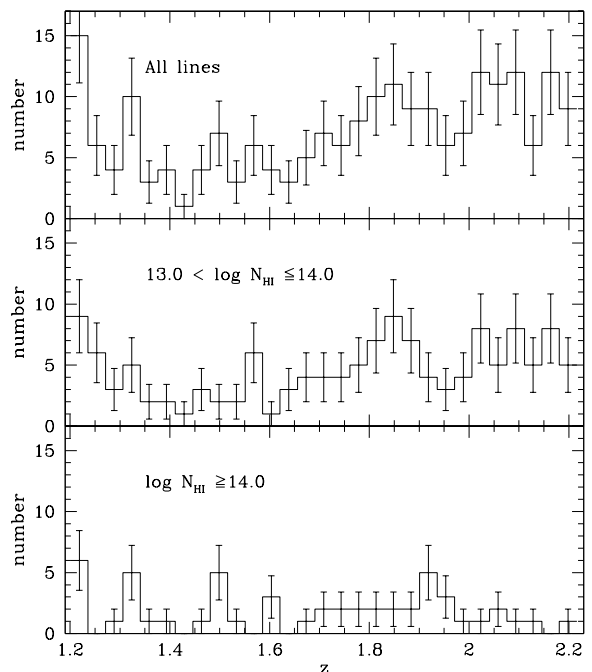


FIG. 2— Histogram of the HI column density of Ly $\alpha$  clouds as a function of redshift for different thresholds. Error bars are the square-root of the number in each bin.

### 3. THE NUMBER DENSITY EVOLUTION AT $Z = 1.20 - 2.20$

The number density evolution of the Ly $\alpha$  forest, described by a power law of the type  $dn/dz \propto (1+z)^\gamma$ , has been studied at high redshift ( $1.7 < z < 4.1$ ) using samples of high resolution data by Giallongo et al. (1996) and Kim et al. (1997). For lines with  $\log N_{HI} \geq 14.0$ ,  $dn/dz$  shows a fast evolution, with  $\gamma \simeq 3.6$ . The analysis at low redshifts (Weymann et al. 1998), based on low resolution spectroscopy of the Quasar Absorption Line Survey (QALS), gives in the range  $0.0 < z < 1.5$  a much flatter  $dn/dz$ , consistent with weak negative evolution (for  $\Omega_o = 1$ )  $\gamma = 0.16 \pm 0.16$ . We note that in the two redshift regimes a variation of  $\gamma$  with column density threshold has been found (larger for increasing threshold). This would go the opposite direction than what is shown in Fig. 2 where  $\gamma$  is smaller for higher threshold. The discrepancy can be explained if a large number of lines with  $\log N_{HI} < 14$  is present, but not detected at  $z = 1.4 - 1.8$ .

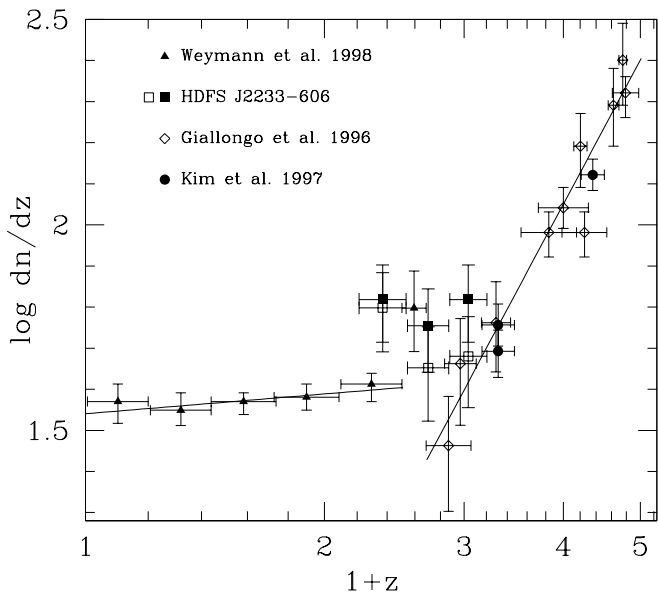


FIG. 3— Number density evolution of the Ly $\alpha$  clouds with  $\log N_{HI} \geq 14.0$  from  $z = 0$  to  $z = 4$ . Filled symbols are for samples that include metal systems, open symbols do not. In the sample of Kim et al., only lines with  $\log N_{HI} \leq 16.0$  are included. The low redshift line is the fit with  $\gamma = 0.16$  obtained by a sample of Ly $\alpha$  clouds with equivalent width  $EW \geq 0.24 \text{ \AA}$  (Weymann et al. 1998) which corresponds to  $\log N_{HI} \geq 14.0$  for  $b \sim 26 \text{ km s}^{-1}$ . The high redshift line is the fit with  $\gamma = 3.62$ .

The problem in comparing high and low redshift data stems from the different techniques used to measure column densities. At high redshifts, high resolution observations allow line fitting of Voigt profiles, and those give more robust results than the curve-of-growth technique used to estimate HI from equivalent width measurements of low resolution data at low redshifts. On the other hand, the strong evolution of line density makes the line deblending of complex structures rather difficult at high redshifts. The Ly $\alpha$  forest of J2233–606 lies between the two redshift regimes and so it is extremely useful to evaluate the correct connection between the two. The results for the two samples of Ly $\alpha$  clouds with and without metal lines are shown in Fig. 3 for lines with  $\log N_{HI} \geq 14.0$ . The

data from J2233–606 have been binned into three redshift ranges  $\Delta z = 1.201 - 1.535$ ,  $1.535 - 1.870$  and  $1.870 - 2.204$  corresponding roughly to the STIS high resolution and medium resolution intervals and to the UCLES high resolution interval. The last two bins give a number density of lines that would better match the high and low redshift observations if metal systems are excluded. The first bin gives a larger number of lines,  $66 \pm 14$  including metal systems, compared with  $40 \pm 4$  lines given the QALS best fit (Weymann et al. 1998). That deviation is not particularly significant, and could indicate a peculiarity along the line of sight to J2233–606. However, a similar excess at  $1.505 < z < 1.688$  ( $63 \pm 14$ ) is also shown by the quasar UM18, which is part of the FOS sample of the QALS, but not included in the fitting of the number density evolution. The excess found in J2233–606 can be due to the presence of a cluster of lines at  $z \sim 1.335$ , as suggested in the previous section. Other possible explanations would be the blending effect by which nearby lines with column density below the threshold would artificially appear in the limited signal-to-noise spectrum as stronger single lines with HI above the threshold, or the presence of a small number ( $\sim 5$  would be enough) of unidentified metal lines interpreted as Ly $\alpha$  lines. This latter possibility looks very unlikely because even in clusters, metal lines typically appear very narrow at high resolution.

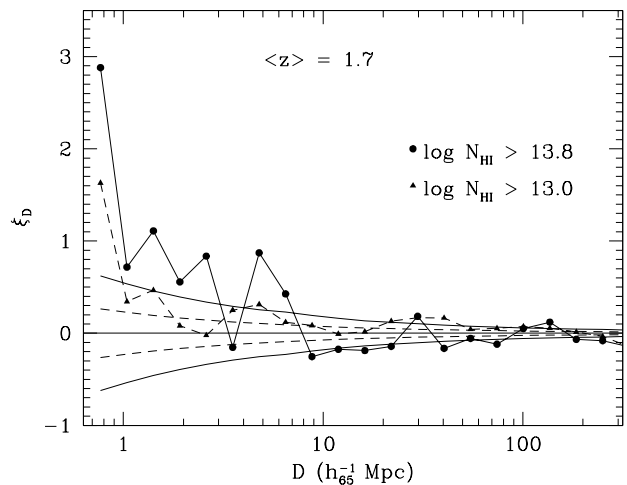


FIG. 4— Two point correlation function of the Ly $\alpha$  forest in J2233–606 for lines with  $\log N_{HI} > 13.0$  and  $13.8$ . The Poisson error is also given as dashed and solid lines respectively.

### 4. THE CLUSTERING PROPERTIES

A positive signal in the clustering properties of the Ly $\alpha$  forest has been found thanks to the advent of high resolution spectroscopy. The investigation has been mainly based on the analysis of the two point correlation function (Cristiani et al. 1997; Kim et al. 1997) but also on that of the power spectrum of mass density fluctuations (Hui et al. 1997; Croft 1998; Amendola & Savaglio 1998). Results have shown that the clustering is present up to  $\Delta v \sim 300 \text{ km s}^{-1}$  and that the amplitude increases with increasing column density threshold of the lines. Most interesting for models of large scale structure formation is the redshift evolution found, showing larger values at smaller redshifts. Although the analysis of the two point correlation function is uncertain when the sample is too

small, we report the result on the forest of J2233–606 in Fig. 4 for two column density thresholds. The signal is significant in the first bin ( $D \sim 0.8 h_{65}^{-1}$  Mpc) and it is higher at the higher HI threshold at about the 6 and 4  $\sigma$  level for  $\log N_{HI} > 13.0$  and 13.8 respectively. In a previous study by Cristiani et al. (1997), the two point correlation function for  $\log N_{HI} > 13.8$  at  $\Delta v = 100 \text{ km s}^{-1}$  has shown a redshift evolution, being  $\xi_{100} \simeq 0.20$  at  $\langle z \rangle = 3.85$  (consistent with no clustering),  $\xi_{100} \simeq 0.75$  at  $\langle z \rangle = 3.40$ , and  $\xi_{100} \simeq 0.85$  at  $\langle z \rangle = 2.40$ . The line of sight of J2233–606 shows  $\xi_{100} \simeq 1.3$  at  $\langle z \rangle = 1.7$  and confirms this evolution.

## 5. THE DOPPLER PARAMETER DISTRIBUTION

Thanks to the high resolution observations of J2233–606, the analysis of the distribution of the Doppler parameter of the Ly $\alpha$  forest can be performed for the first time at these low redshifts. At higher redshifts Kim et al. (1997) have found that the median value of the Doppler parameter is  $b \sim 30 \text{ km s}^{-1}$  at a redshift of  $z \sim 3.7$ , and appeared to increase to  $b \sim 35 - 40 \text{ km s}^{-1}$  at a redshift of  $z \sim 2.3$  for lines with  $13.8 < \log N_{HI} < 16$ , which has been interpreted as an increase of the temperature or kinematic broadening of the clouds. The Doppler distribution in J2233–606 is shown in Fig. 5 for the whole sample and for the subsample of lines (60% of the total) with smaller uncertainties ( $\sigma(b) < 8 \text{ km s}^{-1}$  and  $\sigma(\log N_{HI}) < 0.5$ ). The fit of the two Gaussians (in the interval  $0 < b < 60 \text{ km s}^{-1}$ ) gives in the two cases a mean value of 27 and  $26 \text{ km s}^{-1}$  respectively ( $\chi^2$  is 2.4 and 1.5), and these are slightly different than the median value (29 and  $25 \text{ km s}^{-1}$ ) in the whole  $b$  range. The median values are larger if lines with  $13.8 < \log N_{HI} < 16$  are selected, being  $31 \text{ km s}^{-1}$  in the two cases. Thus, the median value we find over the redshift range  $1.20 < z < 2.20$  is considerably below the value of  $b \sim 40 \text{ km s}^{-1}$  expected on the basis of the redshift evolution suggested by Kim et al. (1997).

## 6. CONCLUSIONS

In contrast to the empty field used for the HDF North program, the HDFs has been selected close to a high redshift quasar, J2233–606 ( $z_{em} = 2.23$ ). The QSO is centered in the STIS field, located approximately 5 and 8 arcmin from the WFPC2 and NICMOS fields respectively. The Ly $\alpha$  forest of J2233–606 has been observed at high and medium resolution (FWHM = 10, 50 and  $8.5 \text{ km s}^{-1}$  in the wavelength intervals  $\lambda\lambda = 2670 - 3040 \text{ \AA}$ ,  $\lambda\lambda = 3040 - 3530 \text{ \AA}$  and  $\lambda\lambda = 3530 - 3900 \text{ \AA}$ ) using STIS/HST (Ferguson et al. 1999) and UCLES/AAT (Outram et al. 1998), giving the opportunity to analyze the properties of the intergalactic medium in the large redshift interval  $z = 1.20 - 2.20$ . This is the first time that the Ly $\alpha$  forest is studied in detail for  $z \lesssim 2$ . More than 200 Ly $\alpha$  cloud redshifts have been found and 63 have HI column density in excess of  $10^{14} \text{ atoms/cm}^{-2}$ , 11 of which have associated metal absorption. The redshift distribution of the lines has shown a deficiency of lines (5 are found over a mean expected of 16) in the interval  $1.383 < z < 1.460$ , corresponding to a comoving size of  $94 h_{65}^{-1} \text{ Mpc}$  ( $\Omega_o = 1$ ). The region around the metal system

at  $z = 1.942$ , also responsible of the Lyman limit observed for  $\lambda < 2700 \text{ \AA}$ , shows an excess of strong lines in the interval  $1.92 < z < 1.99$ , indicating a clustering of Ly $\alpha$  clouds. An excess of lines is also found for  $1.20 < z < 1.38$ . The evolution of the number density in the total sample shows a rapid decrease of lines with redshift. This is partially due to the blending effect of low HI column density lines, which is stronger at lower redshifts. Indeed it tends to disappear when selecting only strong lines ( $N_{HI} \geq 10^{14} \text{ cm}^{-2}$ ). On average the number of strong Ly $\alpha$  clouds per unit redshift is higher than the extrapolation from studies at lower and higher redshifts:  $63 \pm 8$  at  $\langle z \rangle = 1.702$  including metal systems are found to be compared with 41 and 27 expected from the low and the high redshift predictions. A larger sample of lines will confirm if this line density is typical at that redshift or if it is peculiar to the J2233–606 line of sight. The two point correlation function has shown a positive signal up to a scale of the order of  $3 h_{65}^{-1} \text{ Mpc}$ . The amplitude found seems to confirm the evolution with redshift, being larger at lower  $z$ . The mean Doppler parameter of the Ly $\alpha$  forest is around  $26 - 27 \text{ km s}^{-1}$ , corresponding to a temperature, in the case of thermal broadening, of  $\sim 4.3 \times 10^4 \text{ K}$ . The median Doppler parameter evolution reported by Kim et al. (1997) is not confirmed by this Ly $\alpha$  forest.

It is a pleasure to thank L. Amendola, B. Carswell, S. Casertano, G. Ganis, B. Jannuzi, M. Livio, P. Outram and R. Weymann for useful suggestions.

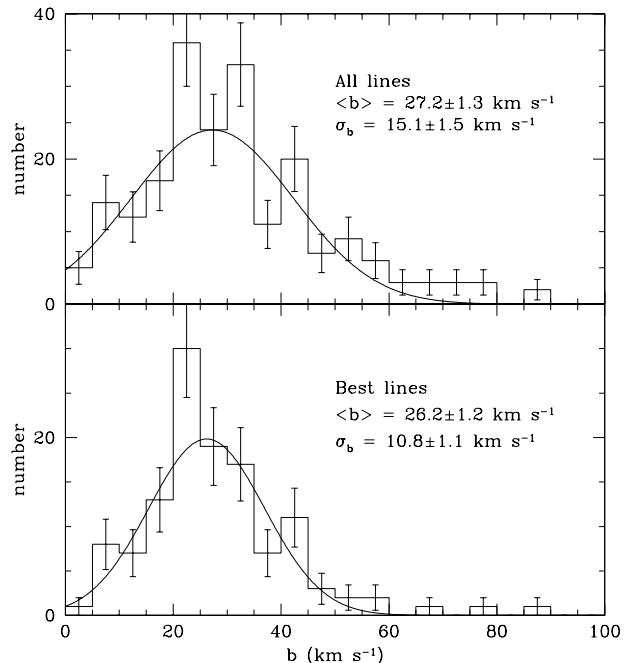


FIG. 5– Doppler parameter histograms of Ly $\alpha$  clouds in J2233–606 in the whole sample (upper panel) or in the subsample of lines with  $1\sigma$  error in the column density and in  $b$  smaller than  $0.5 \text{ dex}$  and  $8 \text{ km s}^{-1}$  respectively (124 lines over a total of 210). The fit of a Gaussian for  $b < 60 \text{ km s}^{-1}$  is shown as well. Error bars are the square-root of the number of lines in each bin.

## REFERENCES

- Amendola L., Savaglio S., 1998, MNRAS, submitted  
Cristiani S., D'Odorico, S., D'Odorico, V., Fontana, A., Giallongo E., Savaglio S., 1997, MNRAS, 285, 209  
Cowie L. L., Songaila A., 1998, Nat, 394, 44  
Croft R. A. C., Weinberg D. H. Pettini M., Hrtquist L., Katz N., 1998, ApJ, submitted, astro-ph/9809401  
Ferguson H. C. et al., 1999, in preparation  
Gardner J. P., 1999, in preparation  
Giallongo E., Cristiani, S., D'Odorico S., Fontana A., Savaglio S., 1996, ApJ, 466, 46  
Fontana A., Ballester P., 1995, The ESO Messenger, 80, 37  
Hui L. Gnedin N. Y., Zhang Y., 1997, ApJ, 486, 599  
Kim T-S, Hu E. M., Cowie L. L., Songaila A., 1997, AJ, 114, 1  
Outram P. J., Boyle B. J., Carswell R. F., Hewett P. C., Williams R. E., Norris R. P., 1998, MNRAS, submitted, astro-ph/9809404  
Savaglio S., 1998, AJ, 116, 1055  
Sealey K. M., Drinkwater M. J., Webb J. K., 1998, ApJL, 499, L135  
Tresse L., Dennefeld M., Petitjean P. et al., 1998, A&A, submitted, astro-ph/9812246  
Weymann R. J., Jannuzi B. T., Lu L., et al., 1998, ApJ., 506, 1  
Williams R. E. et al., 1999, in preparation